Atrazine analysis using an amperometric immunosensor based on single-chain antibody fragments and regeneration-free multi-calibrant measurement

Kathleen Grennan [a], Gillian Strachan [b], Andrew J. Porter [b],
Anthony J. Killard [a], Malcolm R. Smyth [a],*

[a] *National Centre for Sensor Research (NCSR), School of Chemical Sciences, Dublin City University, Dublin 9, Ireland*
[b] *Haptogen Ltd., Polwarth Building, Foresterhill, Aberdeen AB25 2ZD, UK*

Abstract

This work describes the development of an electrochemical immunosensor for the analysis of atrazine using recombinant single-chain antibody (scAb) fragments. The sensors are based on carbon paste screen-printed electrodes incorporating the conducting polymer polyaniline (PANI)/poly(vinylsulphonic acid) (PVSA), which enables direct mediatorless coupling to take place between the redox centres of antigen-labelled horseradish peroxidase (HRP) and the electrode surface. Competitive immunoassays can be performed in real-time using this separation-free system. Analytical measurements based on the pseudo-linear relationship between the slope of a real-time amperometric signal and the concentration of analyte, yield a novel immunosensor set-up capable of regenerationless amperometric analysis. Multiple, sequential measurements of standards and samples can be performed on a single scAb-modified surface in a matter of minutes. No separation of bound and unbound species was necessary prior to detection. The system is capable of measuring atrazine to a detection limit of 0.1 ppb ($0.1 \, \mu g \, l^{-1}$). This system offers the potential for rapid, cost-effective immunosensing for the analysis of samples of environmental, medical and pharmaceutical significance.

1. Introduction

Environmental monitoring has become an increasingly demanding field in recent years, due to both governments and consumers becoming more aware of the damage that can potentially be caused by industrial and agricultural practices. Governments have responded to these concerns by setting guidelines on the maximum permissible levels of pollutants such as pesticides. Atrazine is a member of the *s*-triazine family of herbicides and as such is one of the world's most commonly used pesticides. The European Union Drinking Water Directive set official regulations on the maximum admissible concentration of pesticides such as atrazine in drinking water; namely $0.1 \, \mu g/l$ (0.1 ppb) for an individual pesticide and $0.5 \, \mu g/l$ (0.5 ppb) for total pesticides [1]. In the United States the maximum level of any member of the *s*-triazine class of pesticides permitted in drinking water is $3 \, \mu g/l$ [2]. Due to its widespread use, atrazine is

considered an indicator compound for pesticide pollution and therefore a rapid, reliable, convenient and inexpensive method for its analysis is required.

Many established analytical techniques have been employed for the determination of atrazine in soils and water. These include gas chromatography employing nitrogen–phosphorous detectors [3] or coupled to mass spectrometry [4,5], high performance liquid chromatography with UV-Vis detection [6,7] or coupled to mass spectrometry [8], thin layer chromatography [9] and capillary zone electrophoresis [10]. However, these techniques remain laboratory based and often require extensive sample pre-treatments before they are capable of achieving the required sensitivity. Traditional solid-state immunoassay methods, such as the enzyme-linked immunosorbent assay (ELISA), are also capable of such sensitive measurements [11], but are often unsuitable for on-site analysis, as they can take several hours to complete, they must be performed by trained personnel and require numerous separation and washing steps. These drawbacks, in combination with the cumbersome handling procedures that accompany them, hinder their use as on-site detection systems. Immunosensors combine the sensitivity of the antibody–antigen interaction with the fast, often direct, data acquisition obtainable from biosensor processes [12]. Although several existing optical and piezoelectric immunosensor systems are capable of achieving the required detection limits for atrazine, this is at the expense of experimental complexity and instrumental portability [13,14]. Electrochemical immunosensors, on the other hand, offer a means to miniaturise the analytical system through the use of disposable screen-printed electrodes. Skládal and Kaláb have developed immunosensors based on screen-printed electrodes and amperometric transduction, for the pesticide 2,4-dichlorophenoxyacetic acid (2,4-D) in single electrode [15] and multichannel [16,17] formats. However, these systems required separate incubation and washing steps before detection could be achieved. The principal features of a selection of electrochemical immunosensors for atrazine analysis that have recently been published in the literature are outlined in Table 1.

It has been suggested that the principal limitation of immunosensor technology is related to antibodies and their properties [24]. The majority of environmental, anti-hapten, competition assays are still performed using polyclonal antibodies, largely due to the expenses incurred with monoclonal antibody production [25]. Recombinant antibodies, which are produced using

Table 1
Electrochemical immunosensors for the analysis of atrazine

Detection method	Analysis time (min)	L.O.D. (ppm[a])	Immunoassay format	Reference
Amperometric[b] SPE[c]	15	0.012	Competitive with monoclonal antibodies (glucose oxidase label with HRP for enzyme channelling and catalase for substrate scavenging)	[18]
Amperometric[b] GCE[d]	6–20	4	Competitive with monoclonal antibodies (alkaline phosphatase label)	[19]
Amperometric[b] SPE coated with biotin + streptavidin	20	0.4	Competitive with biotinylated monoclonal antibodies (HRP label)	[20]
Amperometric GCE	5–60	0.001	Competitive (HRP label)	[21]
Amperometric SPE	20–30	1	Direct with monoclonal antibodies (signals amplified with atrazine-tagged liposomes)	[22]
Amperometric GCE	15	0.001	Competitive with polyclonal antibodies (HRP label) 'Molecularly-wired' osmium polymer system	[23]
Amperometric SPE[b]	30	0.001	Competitive with recombinant scAb fragments (HRP label) real-time 'molecularly-wired' PANI/PVS system	Current work

[a] Parts per million ($\mu g\,l^{-1}$).

[b] Flow-based method.

[c] Screen-printed electrode.

[d] Glassy carbon electrode.

recombinant DNA technology, offer the advantages of monoclonal antibodies but at ultimately lower costs [24]. This technology offers a means to produce an infinite supply of antibody fragments, which can be modified to improve the binding properties and stability of the antibody [26]. Apart from reductions in costs, recombinant fragments provide several other advantages for biosensing processes, including the removal of animal sacrifices, decreases in non-specific binding and the advantage of monovalency. Several publications describe the production of such fragments to environmental pollutants but only a few describe the production of fragments to low molecular weight haptens such as the pesticides atrazine [25,27–29], paraquat [25,28] mecoprop [25], diuron [25,30] 2,4-D [31], chlorpyrifos [32] and chlorpyrifos-ethyl [33]. In this work, recombinant single-chain antibody (scAb) fragments to the pesticide atrazine, which have been shown to be capable of as sensitive a detection as their whole antibody counterparts, were employed [28]. Although increasingly employed in traditional immunoassay techniques, the use of recombinant antibody fragments as the sensing material for immunosensors is relatively new. The first and to our knowledge only, electrochemical immunosensor reported to date to use recombinant antibodies has recently been developed by Benhar et al. [34].

An electrochemical immunosensor system based on screen-printed electrodes has been described by Killard and co-workers and has been shown to be capable of the analysis of the vitamin biotin and atrazine [35–37]. A unique advantage of this system over existing electrochemical immunosensors is that it is capable of generating real-time data from concentration-dependent curves. Systems based on real-time biomolecular interaction analysis enable direct detection of antibody–antigen binding events, which can provide important information regarding the affinity and kinetics of antibody–antigen interactions. This data was achieved through the use of mediatorless redox coupling between the electrode surface and the antibody–antigen complexes that are formed on the surface of the conducting polymer polyaniline (PANI). However, this system was not capable of achieving the required limit of detection for atrazine. This may have been due to the batch nature of the experimental protocol and/or the nature of the immunochemicals employed [37].

This work describes the extension of the established competition-based immunoassay format for atrazine analysis to a flow-injection system. Screen-printed electrodes, which were prepared and characterised previously, were employed as the working electrodes [38]. A novel method for the multi-calibrant and multi-competition analysis of analyte is also introduced here, enabling entire calibration experiments to be performed on a single electrode, thereby overcoming problems with inter-electrode variability that are commonly associated with screen-printed electrodes. Several competition immunoassay experiments can also be performed on a single electrode, thereby reducing significantly the time scale of on-site measurements and removing the need to regenerate the antibody-modified surface between analyses.

2. Experimental

2.1. Chemicals

Unless otherwise stated, immunochemicals and chemicals were purchased from Sigma–Aldrich (Poole, Dorset, UK). Anti-biotin antibody was a goat polyclonal (Sigma B3640) and horseradish peroxidase-labelled biotin (biotin-HRP) was biotin-amidocaproyl-labelled peroxidase (Sigma P2907). Single-chain antibody 4D8 fragments to atrazine were prepared from the pIMS 147 vector as described previously [39]. Horseradish peroxidase (HRP) was a gift from Inverness Medical Limited (Inverness, Scotland). 3-Mercaptopropanoic acid was purchased from Lancaster (8479). N-hydroxysuccinimide 85% (w/v) (NHS, 13, 067-2) potassium hydroxide pellets (P 6310), atrazine (45330), sodium hydrogen carbonate (43,144-3), dicyclohexylcarbodiimide (DCC, D8,000-2), dimethylformamide (DMF, 15,481-4), poly(vinylsulphonic acid, sodium salt) (PVS, 27,842-4) and aniline (13,293-4), (vacuum distilled and stored frozen under nitrogen) were all obtained from Sigma–Aldrich. Hydrogen peroxide 30% (v/v) solution (108,597) and absolute ethanol (100,983) were purchased from Merck. Carbon paste No. C10903D14 was obtained from Gwent Electronic Materials Ltd. (Gwent, UK). Silver conductive ink (Electrodag® PF-410) and insulating polymer ink (Electrodag® 452 SS BLUE) were purchased from

Acheson (Plymouth, UK). Poly(ethylene) terephthalate substrates were Melinex films obtained from HiFi Industrial Film Ltd. (Dublin, Ireland).

2.2. Buffers and solutions

PBS is 0.1 M phosphate buffer, 0.137 M NaCl and 2.7 mM KCl, pH 6.8. This was prepared by mixing solutions containing 0.1 M Na_2HPO_4, 0.137 M NaCl and 2.7 mM KCl with a solution of 0.1 M KH_2PO_4, 0.137 M NaCl and 2.7 mM KCl to a pH of 6.8. Unless otherwise stated, all immunochemicals were prepared in PBS.

2.3. Instrumentation

2.3.1. Screen-printed electrode fabrication

Screen-printing was performed with a semi-automated DEK Albany 247 printing machine (Weymouth, UK). A polycarbonate screen with a mesh count of 77 filaments per cm and mounted at $45°$ to the print stroke was employed. Insulation inks were cured using a UV curing system (UV Process Supply Inc., Cortland, Chicago, IL, USA).

2.3.2. General electrochemical experiments

All electrochemical measurements were performed using a BAS100/W electrochemical analyser with BAS100/W software, operating in either cyclic voltammetric, or time-based amperometric modes. Bulk electrochemical experiments employed an Ag/AgCl reference electrode and a platinum mesh auxiliary electrode. A Gilson Minipuls 3 peristaltic pump was employed for flow-injection analysis experiments. The flow cell and miniature batch cell employed have been described previously [35].

2.4. Sensor preparation

Screen-printed electrodes were designed and produced as previously described [38]. Electrodes were cut from the printed sheet leaving excess substrate on either side to a width of 14 mm. Polymerisation of aniline on screen-printed electrode surfaces was carried out potentiostatically as described previously [35]. Immobilisation of protein solutions were carried out as previously described [37]. Two hundred microliters

of antibody solution ($0.5 \mu g \, ml^{-1}$) were used in these immobilisation cases.

2.5. Synthesis of atrazine-HRP conjugate

2.5.1. Derivatisation of atrazine

The synthesis of the carboxylic acid atrazine derivative, 3-{4-(ethylamino)-6-[(1-methylethyl)amino]-1, 3,5-triazin-2-yl} propanoic acid, required for conjugation of atrazine to HRP, was carried out according to Goodrow et al. [40]. A solution of 5.4 mmol 3-mercaptopropanoic acid, 10.8 mmol 85% (w/v) KOH and 10 ml absolute ethanol was added to a stirred homogeneous mixture of 5.01 mmol atrazine and 100 ml absolute ethanol. The mixture was refluxed under nitrogen for 5 h until a white solid remained, which was then taken up in 25 ml of 5% (w/v) $NaHCO_3$. This solution was washed with $3 × 10$ ml quantities of chloroform and acidified to pH 2 with 6 M HCl. The white solid was collected, washed with Milli-Q water and dried. Additional product was obtained through evaporation and crystallisation of the residue from methanol.

2.5.2. Conjugation of atrazine derivative to HRP

Conjugation of the carboxylic acid derivative synthesised in Section 2.5.1 was carried out according to Goodrow et al. [40]. The atrazine derivative was dissolved with equimolar NHS and a 10% (v/v) molar excess of DCC in 1 ml DMF. The mixture was stirred for 3.5 h at room temperature and the precipitated dicyclohexylurea removed by centrifugation. The DMF supernatant was slowly added under vigorous stirring to 200 mg HRP in 5 ml Milli-Q water. The mixtures were stirred at $4°C$ for 22 h until conjugation was complete and subsequently dialysed four times against PBS at $4°C$.

2.6. Electroanalytical procedure

Electrodes that had been immobilised with antibody or enzyme were subjected to the appropriate immunochemical incubations as described subsequently Section 2.7.2. Amperometric experiments were performed at -100 mV versus Ag/AgCl, with a sample interval of 500 ms and at a sensitivity of $1 × 10^{-4}$ A/V.

2.7. Immunoassay procedures

2.7.1. Single electrode analysis

Electrodes were incorporated into a flow-cell set-up as previously described [37]. Following the reaching of a steady state, free atrazine at varying concentrations from 10 to 0.0005 μM, was passed over the surface of the anti-atrazine scAb modified electrode at a flow rate of 400 μl min^{-1} for 30 s. Mixtures of atrazine-HRP at a concentration of 12 μg ml^{-1} and hydrogen peroxide at a concentration of 8 mM were subsequently passed over the surface of the electrode and the amperometric outputs monitored.

2.7.2. Regeneration-free multi-calibrant analysis

2.7.2.1. Multi-calibrant conjugate standard curves.
Electrodes were incorporated into a flow-cell set-up. Mixtures of biotin-HRP or atrazine-HRP at varying concentrations and hydrogen peroxide at a concentration of 8 mM, were passed for intervals of 20 s, over the surface of the antibody-modified electrode at an optimised flow rate of 400 μl min^{-1}. Calibration plots were prepared by plotting the initial linear rate curves against concentration of biotin-HRP or atrazine-HRP.

2.7.2.2. Multi-calibrant competition assays.
Electrodes were incorporated into a flow-cell set-up. Mixtures of atrazine-HRP (0.5 μg ml^{-1}), hydrogen peroxide (8 mM) and varying concentrations of atrazine (0.1–1.0 μg ml^{-1}) were passed for 20 s intervals, over the surface of the antibody-modified electrode at a flow rate 400 μg ml^{-1}. Calibration plots were prepared by plotting the initial linear rate curves against concentration of atrazine.

3. Results and discussion

The electrochemical format employed in these determinations relies on modifications in the activity of the HRP enzyme label. Traditional electrochemical immunosensors achieve this by measuring changes in the binding event after the reaction has gone to completion. Real-time biomolecular interaction analysis on the other hand, enables direct and rapid visualisation of the binding interaction and in so doing, allows information on the fundamental characteristics of the binding process to be elucidated. Such characteristics might include the kinetics of the binding interaction or the concentration of the analyte. In comparison to existing immunosensor methods outlined in Table 1., the present system enables the real-time detection of 0.1 ppb (0.1 μg l^{-1}) atrazine, without the need for lengthy incubation times. Since the system is based on disposable screen-printed electrodes in a flow-injection based system, it is also amenable to miniaturisation and automation.

Due to the small size of haptens, the most frequently employed immunoassay technique for their analysis is the competition immunoassay [41]. A schematic representation of the binding events that take place on the electrode surface during electrochemical immunosensing is shown in Fig. 1. HRP-labelled analyte—in this case atrazine–competes with free antigen for binding to immobilised immunoreagents—in this case the anti-atrazine scAb. In the presence of its substrate, hydrogen peroxide, HRP reacts to induce a flow of electrons from the electrode surface, which is transported through the antibody–antigen complex through the molecular wires of the PANI/PVS copolymer. Unlike traditional immunoassay formats, there is no need to separate bound and unbound antigen, since only redox reactions that are coupled to the electrode surface via the antibody–antigen interaction bond are capable of generating detectable changes in catalytic current. In contrast, uncoupled reactions that take place in solution remove electrons from the bulk electrolyte rather than the electrode surface. The basis of this phenomenon has recently been further elucidated [42].

Using an optimised selection procedure, scAb fragments were isolated from a sheep antibody phage display library and subsequently expressed at low cost and in quantity in *Escherichia coli* (*E. coli*) [39]. They have been shown to be capable of the detection of 1–2 ppt (1–2 ng l^{-1}) of atrazine and demonstrated excellent stability under non-physiological conditions.

3.1. Atrazine analysis using an inhibition immunoassay format

The single electrode analysis format described in Section 2.7.1 was employed to determine the ability of this system to measure atrazine in real time. Free atrazine was introduced into the flow
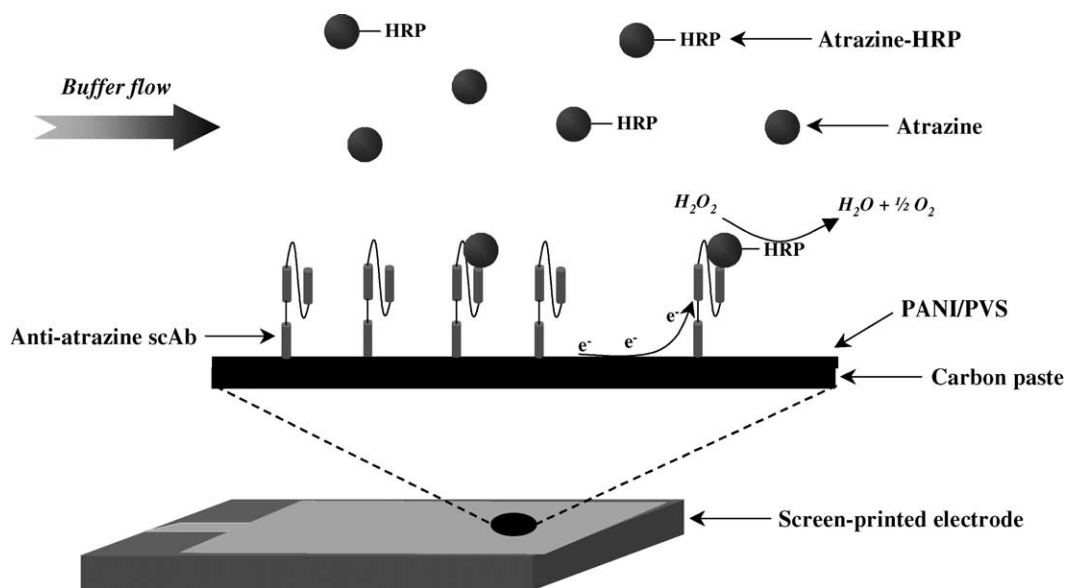
Fig. 1. Schematic diagram of the electrochemical real-time sensing process for atrazine detection. Free and HRP-labelled atrazine compete for binding to immobilised scAb fragments. The interaction of H_2O_2 substrate with HRP produces a catalytic current, which flows from the electrode surface through the molecular wires of the PANI/PVS complex. This response is indirectly proportional to the concentration of bound atrazine.

system for a period of 30 s, followed by mixtures of atrazine-HRP and hydrogen peroxide substrate. This contrasts to the hour long incubations necessary with the quasi-equilibrium format of this system [37]. Fig. 2 illustrates the application of atrazine-HRP, free atrazine and hydrogen peroxide to an anti-atrazine modified electrode in the flow cell. A series of rate curves obtained for varying concentrations of atrazine analyte are given. These are typical of those generated with other real-time formats, in that the rate of response was concentration-dependent, under mass transport limitation conditions. The detection limit of the assay could be controlled by adjusting the period of time the electrode surface was pre-saturated with free atrazine. A period of 30 s at a flow rate of $400 \, \mu l \, min^{-1}$ was adequate to reach the required detection limit of 0.1 ppb ($0.1 \, \mu g \, l^{-1}$).

Using maximum current response data taken at 120 s, the amperometric outputs were inversely proportional to the concentration of free atrazine. When plotted semi-logarithmically, these generated the titration curve shown in Fig. 3 ($n = 3$), which displays the characteristic sigmoidal plot of antibody–antigen interactions typical of competition immunoassay formats. Coefficients of variation (CV) for these measurements ranged from 0.05 to 9%, averaging at 3.4%. These results were comparable to CV values previously reported for atrazine analysis using a real-time batch system [37]. The limit of detection achieved with this system was 0.1 ppb ($0.0005 \, \mu M$), which is in compliance with current EU and world legislations. This system was more sensitive than that previously achieved using the same principle in a batch set-up employing whole monoclonal antibodies to atrazine, which had a detection limit of 28 ppb ($28 \, \mu g \, l^{-1}$) [37]. This poorer detection limit may have been due to the larger cell volume of $200 \, \mu l$ in the batch set-up, which may have introduced mass transport limitations into the system, consequently adversely affecting the sensitivity. The use of a thin layer cell and flow injection process significantly improves mass transport characteristics, thereby increasing the sensitivity of the assay. In addition, the use of monovalent scAb fragments in the place of bivalent antibodies may increase the number of binding sites per unit area.
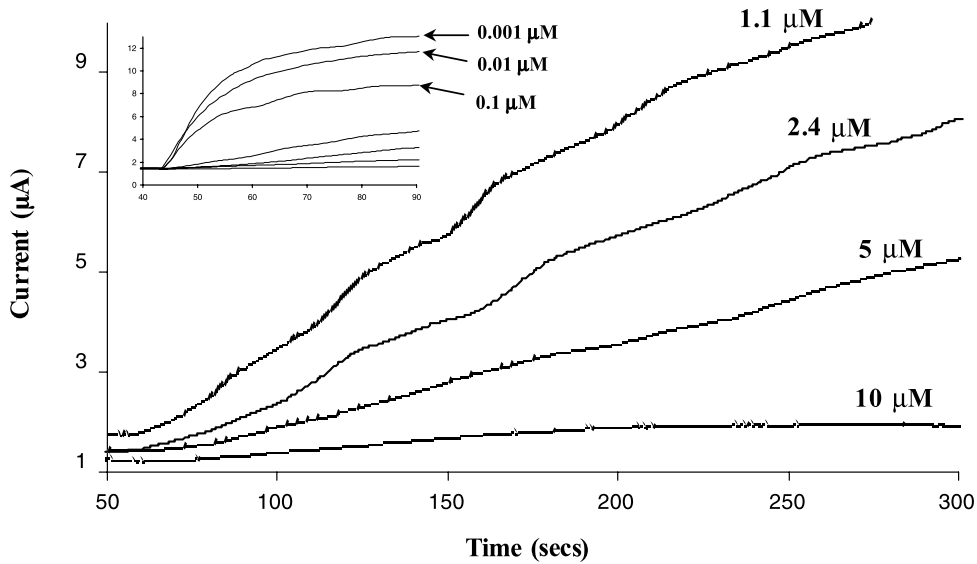
Fig. 2. Typical rate curve responses for a competition immunoassay between atrazine and atrazine-HRP for binding to an electrode modified with scAb to atrazine. The slopes of the amperometric responses decreased with increasing atrazine concentration. The main graph shows atrazine concentrations between 1.1 and 10 μM. Inset shows atrazine concentrations from 0.001 to 10 μM (−100 mV vs. Ag/AgCl).

3.2. Regeneration-free multi-calibrant analysis

One of the most regularly cited problems with screen-printed electrodes is their lack of reproducibility. This can result from the lack of control on the character of the electrode's microscopic structure, re-sulting in different surface morphologies of the working electrodes [43]. Due to the nature of the printing process, no two screen-printed electrode surfaces can be considered identical, even if printed in the same batch. Although electrochemical pre-treatment using a single cyclic voltammetric sweep in sulphuric
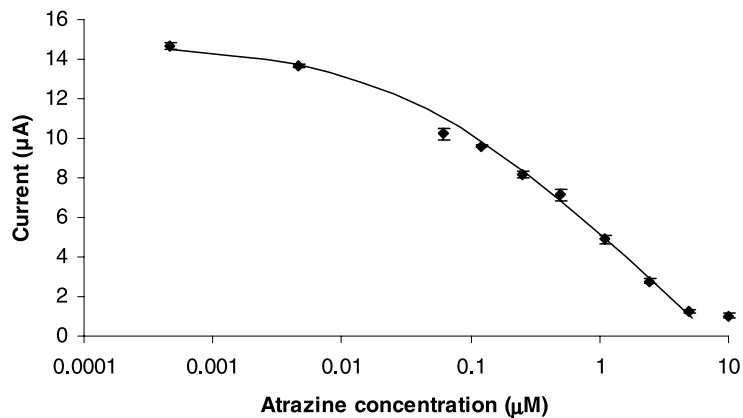

Fig. 3. Inhibition immunosensor assay for atrazine. Current responses were derived from maximum current responses at 120 s. An analytical range of atrazine between 0.12 and 5 μM was established, with a limit of detection of 0.1 ppb (0.0005 μM) ($n = 3$) and CV's ranging between 0.05 and 9%.

acid solution has been shown to have the effect of minimising these inter-electrode variabilities, structural and hence electrochemical differences between screen-printed electrode surfaces inevitably prevail [38]. Such inter-electrode variabilities can theoretically influence all electrochemical measurements irrespective of the electrode material, with the possible exception of mercury electrodes, which generate renewable electrode surfaces for each successive measurement. An alternative approach to the experimental methodology was sought in order to overcome rather than minimise inter-electrode variabilities.

Rather than measure the maximum current response obtained after an immunosensing assay, quantitative measurements can also be made by observing the change in signal after a specific period of time has elapsed. Alternatively, the rate at which interaction occurs can be determined from the slope of the increase in signal, where slope is related to concentration. When measurements are performed based on maximum current responses, normally a single measurement has to be made on the surface before the surface must be renewed by removing one or both of the interacting species in a regeneration process. This is because the surface becomes saturated after a period of interaction (in this case, less than a minute) and the linear relationship between concentration and signal breaks down. Normally, several standards need to be prepared for a standard curve and also several samples often need to be measured. There are many reasons why regeneration of the antibody-coated surface may not be desirable. Due to the strength of the antibody–antigen interaction, harsh conditions are required to break them. Such conditions include the use of solutions of high or low pH, chaotropic agents, proteases and high salt concentrations [12]. These procedures may not only cleave the bonds between the immunocomplex, but can also denature the immobilised antibody and/or damage the sensor surfaces irreparably. Consequently a trade-off exists between sensitivity and repeatability. In addition, the need for regeneration steps can add significantly to the time taken to perform a measurement. Removal of regeneration through the performance of multiple measurements sequentially on a single surface based on measurements on changes in slope could bring many advantages. Several samples could be analysed on a single electrode, thereby decreasing sensor

preparation times, as well as analysis times and costs by several factors.

As a biomolecular interaction occurs at a transducer surface, it proceeds to saturation at a rate of $R \sim t^{1/2}$, where R is the response and t refers to time. This is a non-linear response. However, in the initial portion of a signal, when t is small, the relationship between R and t is pseudo-linear and can be approximated as such. Thus, at sub-saturation of the transducer surface, a linear relationship holds between concentration and slope. In this region, multiple sample applications and measurements can be made, as long as they remain within the pseudo-linear region. Several standards and samples can be analysed on a single surface in this way and calibration curves established from which to calculate unknowns. These can be performed very quickly (second time scales) and in quick succession, resulting in rapid, multi-calibrant analysis.

By employing flow-injection to pass a series of biotin-HRP standards over one electrode surface and extracting kinetic rate data (Fig. 4(a)), a single standard curve could be obtained (Fig. 4(b)). Rate data was extracted from the first 15–20 s of the response, which corresponded to between thirty and forty data points. These generated rate curves which bear the same concentration/rate relationships as previous real-time responses obtained on sequential electrodes, with correlation coefficients (r^2) of greater than 0.99 for each slope. This self-calibration of each electrode overcomes irreproducibility and inter-electrode variability by subjecting all samples to the same system. Use of the single electrode assay provides a regenerationless system, with the possibility of analysing samples and standards on a single antibody-modified surface.

This system was further extended to the analysis of atrazine-HRP standards and a similar series of kinetic responses was obtained as shown in Fig. 5. Significantly lower sample concentrations of $0.05\,\mu g\,ml^{-1}$ analyte were capable of being analysed in this case, compared to $10\,\mu g\,ml^{-1}$ with the whole IgG biotin system. This was attributed to the greater binding affinities of the scAb fragments and their decreased steric hindrance effects on the electrode surfaces. Responses from repeated multi-calibrant measurements were normalised to the slope (m) of the first response, in this case the slope of the $0.05\,\mu g\,ml^{-1}$ response ($m_{0.05}$). This method allows calibration curve results constructed from different electrodes to be compared.
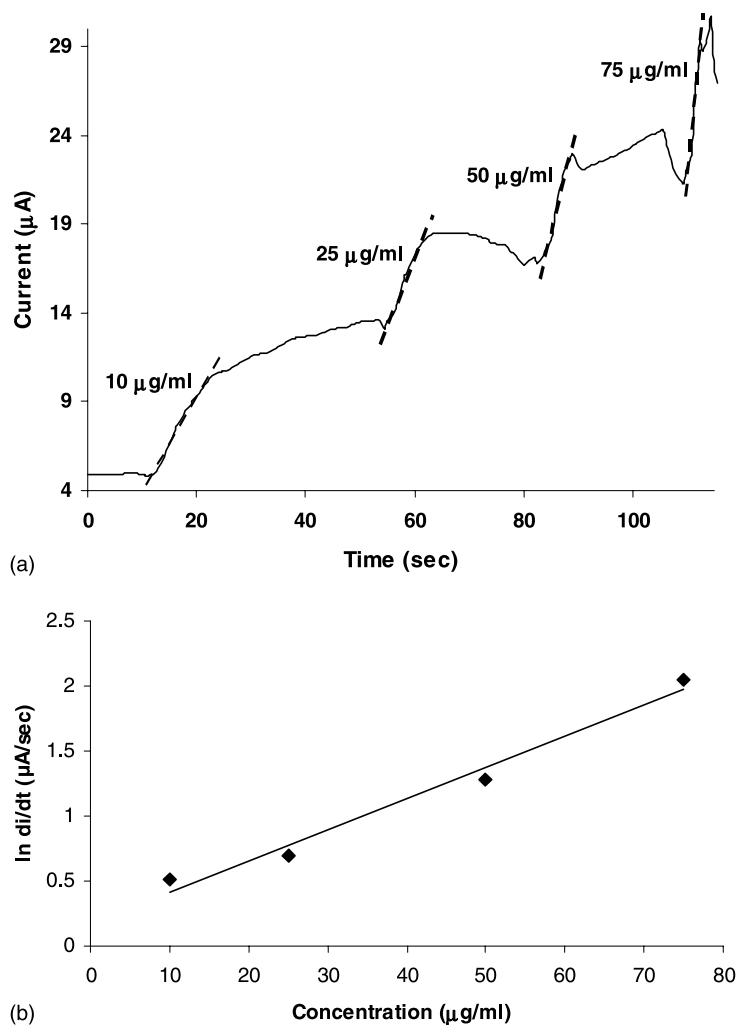
(a)

(b)

Fig. 4. Multi-calibrant analysis of biotin-HRP on a single electrode surface. Biotin-HRP standards from 10–75 μg ml^{-1} were passed over the electrode (a). Initial linear rates were plotted (dotted lines) yielding calibration curves of biotin-HRP concentration (b). Equation of line: $y = 0.0239x + 0.1783$, $r^2 = 0.9783$.

The normalised plot for this calibration, obtained from measurements on three different electrodes, is given in Fig. 5(c). CV's were below 1.5% for each datum, illustrating that the multi-calibrant system holds irrespective of inter-electrode or sensor variabilities.

A competition assay for atrazine was set up with mixtures of atrazine, atrazine-HRP and hydrogen peroxide substrate introduced into the system in a single step. This contrasts to the sequential additions employed for the single electrode analysis described in

Section 2.7.1, which had previously been employed with this flow system [34]. Responses typical of that shown in Fig. 6 were obtained, with the expected inverse relationship between free atrazine concentration and the slope of the response. It also proved possible to re-introduce lower concentrations of atrazine after higher concentrations, proving that the system had not become saturated after a series of successive measurements. A calibration range between 0.02 and 0.22 μM could be achieved using this methodology.

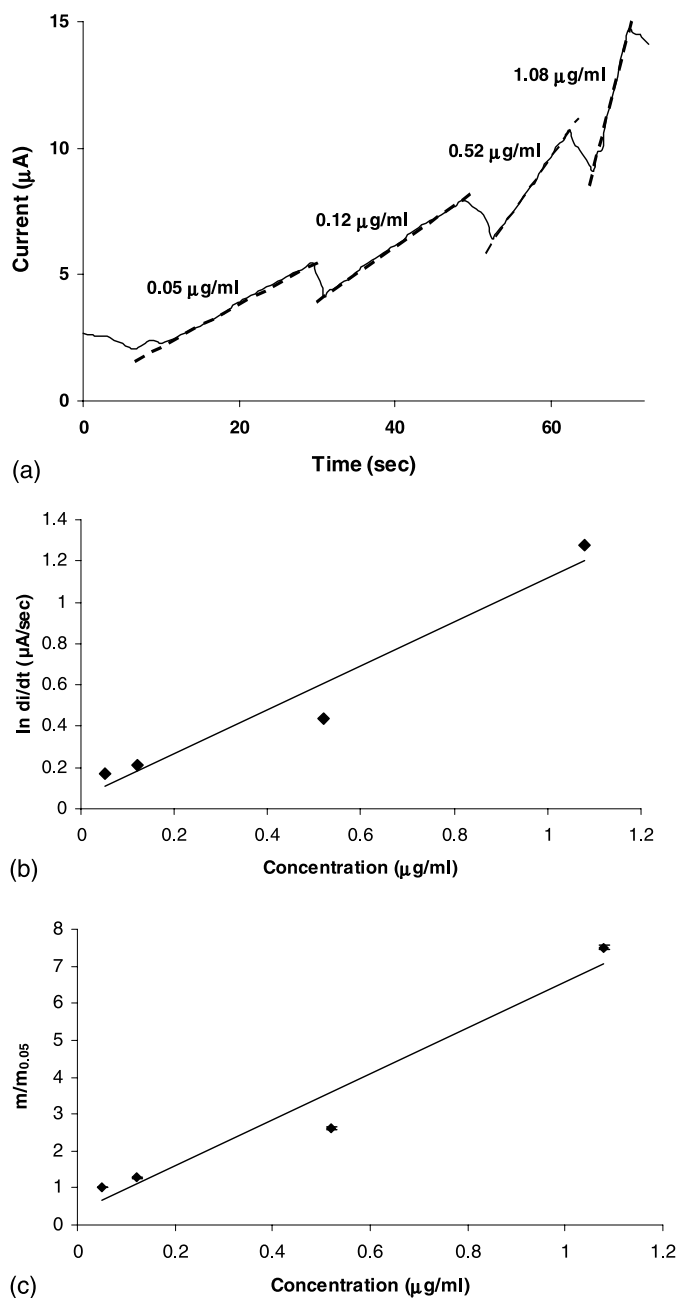Fig. 5. Multi-calibrant analysis of atrazine-HRP on a single electrode surface. Atrazine-HRP standards from 0.05–1.08 μg ml^{-1} were passed over the electrode (a). Initial linear rates were plotted (dotted lines) yielding calibration curves of atrazine-HRP concentration (b). Equation of line: $y = 0.0239x + 0.1783$, $r^2 = 0.9783$. Normalised responses whereby each rate was ratioed relative to the slope of the 0.05 μg ml^{-1} response, yielded a similar calibration curve (c). Equation of line: $y = 6.2443x + 0.3389$, $r^2 = 0.9534$.
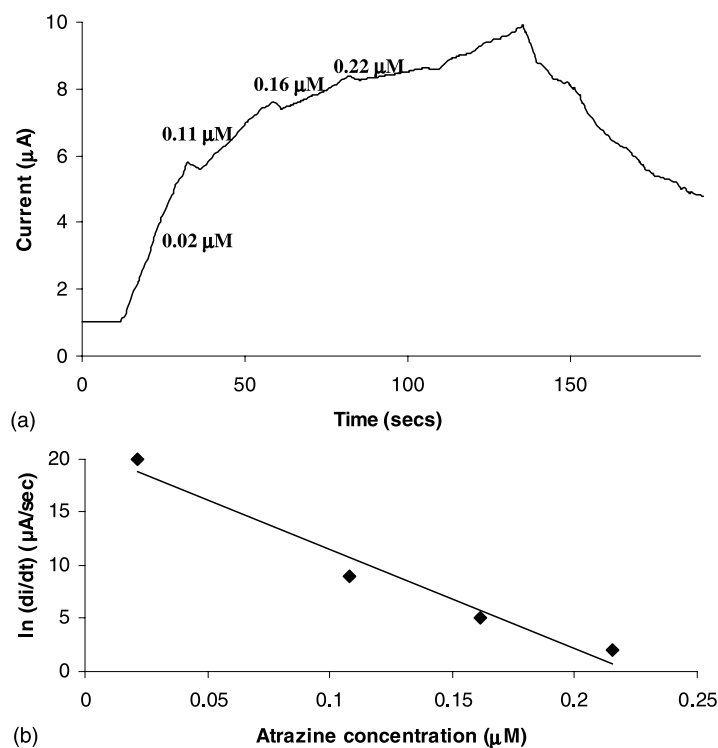
Fig. 6. Kinetic rate curve for a competition immunoassay for atrazine on a single anti-atrazine scAb coated screen-printed electrode (a). The surface was not saturated after the 2 min experiment, as it was still possible to re-introduce samples with lower atrazine concentrations (viz. 0.11 μM in (a)) after the experiment had been completed. The slopes of the responses were used to construct the calibration curve shown in (b). A calibration range between 0.02 and 2 μM was achieved. Equation of line: $y = -93.456x + 20.833$, $r^2 = 0.9638$.

4. Conclusions

The immunosensor described has been shown to be capable of the real-time analysis of atrazine using a competition immunoassay format. Through integration of an established PANI/PVS system with flow injection analysis and replacement of whole immunoglobulins with single-chain antibody fragments as the sensing element, detection limits for atrazine have been lowered to 0.1 ppb ($0.1\,\mu g\,l^{-1}$), which complies with current European Union and world legislations. Single-electrode multi-calibrant analysis has also been shown to be a promising new direction for real-time analysis and reveals the potential of this system for regeneration-free analysis of a series of samples and standards on a single electrode surface. In comparison to existing immunosensor systems for atrazine, this system has demonstrated the potential for repeated measurements to be performed on a single electrode surface. In addition, all reagents can be introduced into the system in a single step, thereby removing the need for time-consuming incubations. Systems employing this format will ultimately lead to reductions in analysis times, sample volumes and inter-electrode variabilities. Since the system is based on disposable screen-printed electrodes in a flow-injection based system, it is also amenable to miniaturisation and automation.

In its present format this immunosensor is suitable as a disposable test for single use by both regulatory authorities and industries for routine testing and screening or for testing of areas suspected of being polluted. The quantitative or semi-quantitative analysis obtainable from this system can enable remedial action to be subsequently taken, whereupon suspect samples could then be sent to a central laboratory for a more extensive analysis by established analytical techniques.

Acknowledgements

References

[1] EU Directive 80/778/EEC, Commission of the European Union, 1980.

[2] US Environmental Protection Agency, National survey of pesticides in drinking water wells, phase II report, EPA 570/9-91-020, National Technical Information Service, Springfield, VA, 1992.

[3] H. Sabik, R. Jeannot, J. Chrom. A 818 (2) (1998) 197.

[4] J. Quintana, I. Martí, F. Ventura, J. Chrom. A 938 (1–2) (2001) 3.

[5] E.M. Thurman, M. Meyer, M. Pomes, C.A. Perry, P. Schwab, Anal. Chem. 62 (18) (1990) 2043.

[6] A. Balinova, J. Chrom. A 643 (1–2) (1993) 203.

[7] R. Carabias-Martínez, E. Rodríguez-Gonzalo, E. Herrero-Hernández, F.J. Sánchez-San Román, M.G.P. Flores, J. Chrom. A 950 (1–2) (2002) 157.

[8] D. Barcelo, G. Durand, V. Bouvot, M. Nielen, Environ. Sci. Technol. 27 (1993) 271.

[9] U. De La Vigne, D.E. Jänchen, W.H. Weber, J. Chrom. A 553 (1991) 489.

[10] K.V. Penmetsa, R.B. Leidy, D. Shea, J. Chrom. A 745 (1–2) (1996) 201.

[11] T.J. Giersch, Agric. Food Chem. 41 (1993) 1006.

[12] P. Skládal, Electroanalysis 9 (10) (1997) 737.

[13] M. Minunni, M. Mascini, Anal. Lett. 26 (7) (1993) 1441.

[14] G.G. Guilbault, B. Hock, R. Schmid, Biosens. Bioelect. 7 (1992) 411.

[15] T. Kaláb, P. Skládal, Anal. Chim. Acta 304 (1995) 361.

[16] P. Skládal, T. Kaláb, Anal. Chim. Acta 316 (1995) 73.

[17] T. Kaláb, P. Skládal, Electroanalysis 9 (1997) 293.

[18] R.W. Keay, C.J. McNeil, Biosens. Bioelect. 13 (1998) 963.

[19] F. Vianello, L. Signor, A. Pizzariello, M.L. Di Paolo, M. Scarpa, B. Hock, T. Giersch, A. Rigo, Biosens. Bioelect. 13 (1) (1998) 45.

[20] J.M. Fernández Romero, M. Stiene, R. Kast, M.D. Luque de Castro, U. Bilitewski, Biosens. Bioelect. 13 (1998) 1107.

[21] J. Parellada, A. Narváez, M.A. López, E. Domínguez, J.J. Fernández, V. Pavlov, I. Katakis, Anal. Chim. Acta 362 (1998) 47.

[22] A.J. Bäumner, R.D. Schmid, Biosens. Bioelect. 13 (1998) 519.

[23] M.A. López, F. Ortega, E. Domíguez, I. Katakis, J. Mol. Recog. 11 (1998) 178.

[24] B. Hock, Anal. Chim. Acta. 347 (1997) 177.

[25] G. Strachan, J.A. Whyte, P.M. Molloy, G.J. Paton, A.J.R. Porter, Environ. Sci. Technol. 34 (2000) 1603.

[26] H.M.E. Azzazy, W.E. Highsmith Jr., Clin. Biochem. 35 (2002) 425.

[27] V.K. Ward, P.G. Schneider, S.B. Kreissig, B.D. Hammock, P.V. Choudary, Protein Eng. 6 (8) (1993) 981.

[28] M. Longstaff, C.A. Newell, B. Boonstra, G. Strachan, D. Learmonth, W.J. Harris, A.J. Porter, W.D.O. Hamilton, Biochim. Biophys. Acta 1381 (2) (1998) 147.

[29] G. Strachan, S.D. Grant, D. Learmonth, M. Longstaff, A.J. Porter, W.J. Harris, Biosens. Bioelect. 13 (1998) 665.

[30] K.B.G. Scholthof, G. Zhan, A.E. Karu, J. Agric. Food Chem. 45 (1997) 1509.

[31] M. Gerdes, M. Meusel, F. Spener, J. Immunol. Methods 223 (1999) 217.

[32] M.J. Alcocer, C. Doyen, H.A. Lee, M.R. Morgan, J. Agric. Food Chem. 48 (2) (2000) 335.

[33] M.J. Alcocer, C. Doyen, H.A. Lee, M.R. Morgan, J. Agric. Food Chem. 48 (9) (2000) 4053.

[34] I. Benhar, T. Eshkenazi, T. Neufeld, J. Opatowsky, S. Shaky, J. Rishpon, Talanta 55 (2001) 899.

[35] A.J. Killard, S. Zhang, H. Zhao, R. John, E.I. Iwuoha, M.R. Smyth, Anal. Chim. Acta 400 (1999) 109.

[36] A.J. Killard, M.R. Smyth, K. Grennan, L. Micheli, G. Palleschi, Biochem. Soc. Trans. 28 (2) (2000) 81.

[37] A.J. Killard, L. Micheli, K. Grennan, M. Franek, V. Kolar, D. Moscone, I. Palchetti, M.R. Smyth, Anal. Chim. Acta 427 (2001) 173.

[38] K. Grennan, A.J. Killard, M.R. Smyth, Electroanalysis 13 (8–9) (2001) 745.

[39] K. Charlton, W.J. Harris, A.J. Porter, Biosens. Bioelect. 16 (2001) 639.

[40] M.H. Goodrow, R.O. Harrison, B.D. Hammock, J. Agric. Food Chem. 38 (1990) 990.

[41] P. Tijssen, Practice and Theory of Enzyme Immunoassay, Elsevier, Oxford, 1985.

[42] A. Morrin, A. Guzman, A.J. Killard, J.M. Pingarron, M.R. Smyth, Biosens. Bioelect. 18 (2003) 715.

[43] C.A. Galán-Vidal, J. Muñoz, C. Domínguez, S. Alegret, Trends Anal. Chem. 14 (5) (1995) 225.